

Analyzing 3D Cell Data of Optical Diffraction Tomography through Volume Rendering

Taeho Kim, Jinah Park

Korea Advanced Institution of Science and Technology (KAIST)

Daejeon, Korea

kdhtheo@kaist.ac.kr, jinahpark@kaist.ac.kr

Abstract—Optical diffraction tomography (ODT) constitutes a novel approach for acquiring cell images since it is capable of capturing morphology of a living cell without chemical treatment. ODT is an interferometric technique that measures the 3D refractive index (RI) distribution of optically transparent samples such as biological cells. Unlike other cell imaging modalities, naïve ODT data do not contain encoded information about the cellular properties such as labeled protein in fluorescent microscopic data or the fixed border of a cell wall in scanning electron microscopic data. Therefore, specifying the region of interest in the raw image is an important and challenging task for a quantitative analysis of ODT cell data.

We propose an interactive interface for reconstructing 3D shape of cells from ODT image data based on intervening visualization results of the cell data to guide the investigator observing the overall blueprint of cell morphology. The cell organelles are segmented based on the lookup table referring corresponding transfer function items adopted from volume rendering technique. The final shape of the cell is then constructed as mesh models from the segmentation results for further quantitative analyses. In this paper, we also demonstrate the various modeling options accounting characteristics of target cell.

Keywords—Optical diffraction tomography; Living cell image; Modeling; Interface; Volume quantification

I. INTRODUCTION

Quantitative analysis as well as observation of the characteristics of biological cells and tissues is crucial in the field of biology and medicine. Cell morphology and its internal structures are widely investigated in the studies of stem cells, cancer cells, and blood cells, for examples. Since morphological information is important to understand the cellular organization and the state of the cells, it can be used as a measure of various biological assays. The examinations of the cell behavior require quantitative measures on curvature, area, perimeter, eccentricity or a categorization of the nuclear type for a large population of cells. For successful studies, the acquisition of specific structures from the original specimen is important and challenging task in cellular imaging.

Conventional bright-field optical microscope represents the projection of transparent object and it is hard to detect desired organelles mainly due to a low contrast in the image. To visualize appearance of the cell as precisely as possible,

several types of imaging techniques were proposed. To delineate a shape of the cell, electron microscopy (EM) uses a coating on samples using a metal or a carbon with various configurations depending on the application. On the other hand, fluorescent microscopy (FM) stains a specimen to increase contrast through changing the color of some parts of the target allowing a clearer view of the cell structure. Both imaging techniques facilitate capturing the appearance of the cells with high resolution. While FM enables sub-diffraction-resolution imaging [1, 2, 3], EM has achieved the resolution of near-atomic dimension [4]. However, their sample preparation procedures are very time consuming and user-dependent. More importantly, the prepared samples are no longer alive in the process, and the use of exogenous labels such as fluorescence proteins or dyes inevitably cause unwanted effects to the physiology of cells.

Optical diffraction tomography (ODT) evades these limitations in bio-imaging, and enables dynamic 3D imaging of intact biological cells and tissues [5, 6]. Recently, ODT has become widely used in various disciplines in biology and medicine, due to its non-invasiveness and quantitative imaging capability [7, 8, 9]. Exploiting digital holographic recording and the principle of inverse light scattering, ODT reconstructs 3D complex refractive index (RI) maps of live biological cells, contacting information about both the light absorptivity and the phase retardation [10]. Hence, for the visualization of ODT data, the real part of RI is unusually shown as the brightness [11]. Because ODT does not provide molecular-specific information, the resulting image consists of voxels containing different RI values without labels and specific cell structures are not always separable automatically.

In this paper, we present an effective interface for reconstructing 3D shape of cell components from the ODT cell image data. We also develop a virtual staining tool resulting FM-like volume visualization as well as segmentation of the cell components.

II. VOLUME SEGMENTATION FROM VISUALIZATION RESULT

To handle volumetric image data, an experimenter usually performs the task of segmentation to identify the regions of interest from the original image. To expedite the process, several automatic segmentation techniques of internal cell structures were proposed for stained cell image [12]. However, for the ODT data, it is hard to apply such techniques directly due to fuzzy boundaries that represent each of cell structures. Furthermore, the boundary of the cellular structure is fluidic, so that it is difficult to define it with a fixed shape. Fig 1 shows two different appearances of the same cell – one is of label-free ODT and the other a stained image. The stained image highlights specific organelle of the cell (the nuclei labeled with DAPI) while ODT contains the holistic information of the cell (NIH 3T3 mouse embryonic fibroblast cell [13]).

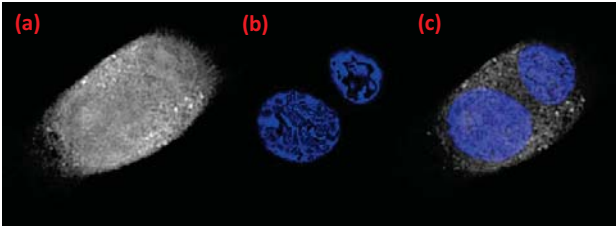


Fig 1. NIH 3T3 mouse embryonic fibroblast cell image: (a) 2D slice of ODT (b) 2D slice of fluorescence tomography with stained nuclei (c) Overlay of the images from both modalities

We develop an interactive visualization tool which mimics the staining process of the fluorescent microscopy using medical imaging toolkit (MITK) open source library [14]. The volume rendering with 2D transfer function [15] is adopted to emphasize the border of the cell. The user can define a set of custom transfer functions to visualize the desired region of the original image.

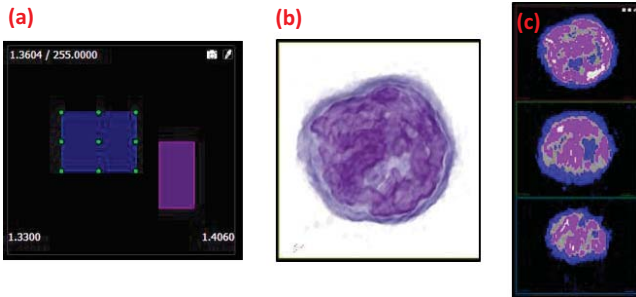


Fig 2. Interactive visualization interface for ODT cell image: (a) Virtual palette to handle user-defined 2D transfer functions (b) 3D render window for visualizing the volume rendering result (c) 2D render windows for illustrating three orthogonal planes of the volume data

Figure 2 shows a snapshot of the process for segmentation of ODT data of white blood cell (B-cell) [16]. In Fig 2 (a), the rectangles represent a user-defined transfer function where the width and the height of the rectangle denote a range of the RI and a range of the image gradient magnitude (GM), respectively. The user can modify the color or adjust

the width and the height by manipulating control points colored in green. For each set of voxels that lies within the corresponding transfer function, the visualization results are updated to the virtual environment named “render window” accordingly. The user observes both 3D volume rendered image (Fig 2(b)) and a set of 2D segmentation results of three orthogonal slices (Fig 2(c)). By fine-tuning the transfer function interactively in the virtual palette consulting the volume rendered image reflecting the changes immediately, the user can obtain desired segmentation results used for the modeling process to follow.

III. MODELING OF CELL STRUCTURES

When we visualize the segmented results by the selected regions of 2D transfer functions, we often see that the voxels are sparsely scattered. In other words, for many cases, the ranges of RI and gradient magnitudes do not provide a fully-filled region of a desired structure. In this section, we introduce a method for constructing a 3D shape model for cell structures by classifying the model in the following three types: a model with scattered multiple components, a closed single model, and a model with hierarchical subparts.

Model having scattered multiple components

The components of the cell which have high RI value and are large in number tend to be located at the diverse position of the cell. It is relative easy to extract a set of the organelles since they usually have a distinct RI values compared to surrounding structures. We define the set as a whole as a model having multiple components. For example, as shown in Fig 3, the lipid droplets of the hepatocyte (Huh-7 [17]) cell were successfully modeled from the segmentation results without any post-processing.

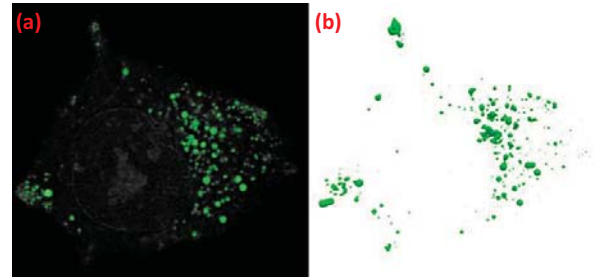


Fig 3. Lipid droplets in Huh-7 cell (liver cell): (a) Converted volume segments from a visualization result (b) Generated mesh models from the segmentation

Closed single model

In Fig 4 (b), the volume rendering result is acceptable for representing a shape of red blood cell (RBC), however, in Fig 4 (a) the segmentation consists of a fuzzy set of voxels. Even the initial segmentation have missing information for the closed region of the cell structure; the resulting model forms a single mesh model.

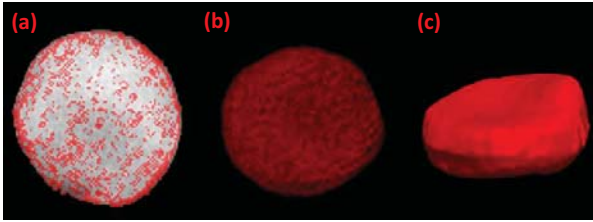


Fig 4. Red Blood Cell (RBC) data: (a) Converted volume segments from a visualization result (b) Volume rendering result (c) Generated mesh model from the segmentation with post-processing

In this study, we implement automatic morphological operations to supplement missing information from the initial segmentation [18]. Figure 4 shows the RBC model generated from segmentation after applying a post-processing method to fill holes.

Model having hierarchical subparts

The most of the cell has multi-structure with several organelles. Moreover, a single specimen may contain two or more cells in clinical analysis. For example, in Fig 5 (e), there are four HeLa cells in the image, and each cell contains many sub-structures in it. Fig 5 (f) shows three transfer functions representing properties of sub-structures. Since the transfer function has RI and gradient range information associated with the whole volume, it handles the segmentation as one object even though there are more than one component of the cell. In other words, we cannot distinguish four cells using the transfer function items.

To organize the quantitative resources from ODT cell image systematically, we define the mutual relationship among models of cell structure. The cell structure which is located inside of the other structure is automatically labeled as a sub-component. By defining the model as a hierarchical model with multi-labeled set of shapes, the computed information of the cell can be examined and handled better. The label may refer to a cell-wise numbering or an inner structure classification as shown in Fig 5 (d).

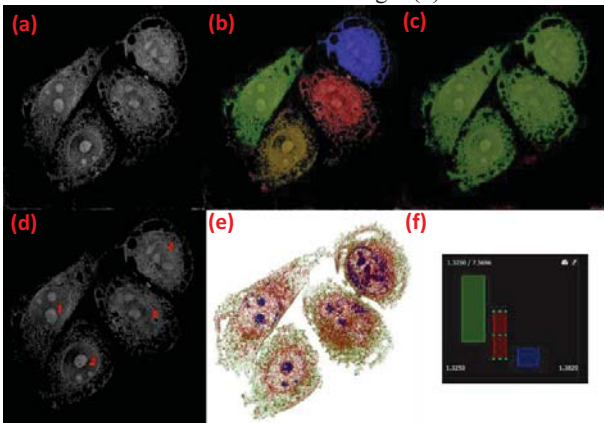


Fig 5. HeLa cell data: (a) Original ODT (b) Highlighted cell area with cell-wise estimated segmentation (c) Background removal based on selected cells (d) Labeling result of the cells (e) Volume rendering result (f) Virtual palette for transfer functions

IV. CONCLUSION

We proposed an interactive interface for modeling cell structures from ODT image data based on visualization results which guide a user by providing visual feedbacks along with semi-automatic supplemental functionalities to improve efficiency in the computer-aided diagnosis in biological studies. In this paper, we demonstrated the modeling results of the cell components of the various kinds of cells.

Figure 6 depicts a volume rendering of cell structures which show nearly transparent property. We see that the voxels identified as a part of the cell are scattered in the slice of the segmentation result. (See the colored voxels in Fig 6 (b).) As the level of sparsity increases, it becomes impossible to identify or unify these voxels as a structure. The additional information to be considered in the modeling process needs to be investigated further. We are currently working on improving the interface by adding a trim process for combining seed segmentation and higher level information.

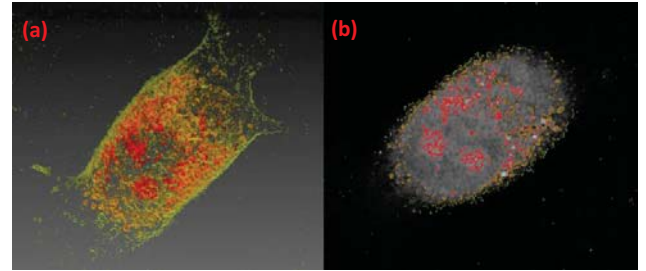


Fig 6. NIH 3T3 mouse embryonic fibroblast cell image: (a) Volume rendering result (b) A slice of image showing a lack of information for the modeling

ACKNOWLEDGEMENTS

This research was supported by Basic Science Research Program through the National Research Foundation of Korea (NRF) funded by the Ministry of Science, ICT and Future Planning (NRF-2016R1A2B4014628). We thank Tomocube Inc. for ODT data sets used for our experiments.

REFERENCES

- [1] B. Lounis, W. E. Moerner, "Single photons on demand from a single molecule at room temperature", *Nature* 407(6803), 491-493, 2000
- [2] E. Betzig, G. H. Patterson, R. Sougrat, O. W. Lindwasser, S. Olenych, J.S. Bonifacio, H. F. Hess, "Imaging intracellular fluorescent proteins at nanometer resolution", *Science*, 313(5793), 1642-1645, 2006
- [3] T. A. Klar, S. Jakobs, M. Dyba, A. Egner, S. W. Hell, "Fluorescence microscopy with diffraction resolution barrier broken by stimulated emission", *Proceedings of the National Academy of Sciences*, 97(15), 8206-8210, 2000
- [4] W. Kühnbrandt, "The resolution revolution", *Science* 343(6178), 1443-1444, 2014
- [5] E. Wolf, "Three-dimensional structure determination of semi-transparent objects from holographic data," *Optics Communications* 1, 153-156 (1969).

- [6] K. Kim, J. Yoon, S. Shin, S. Lee, S.-A. Yang, and Y. Park, "Optical diffraction tomography techniques for the study of cell pathophysiology," *Journal of Biomedical Photonics & Engineering* 2, 020201 (2016).
- [7] K. Kim and Y. Park, "Tomographic active optical trapping of arbitrarily shaped objects by exploiting 3D refractive index maps," *Nature Communications* 8(2017).
- [8] S. Lee, H. Park, K. Kim, Y. Sohn, S. Jang, and Y. Park, "Refractive index tomograms and dynamic membrane fluctuations of red blood cells from patients with diabetes mellitus," *Scientific Reports* 7(2017).
- [9] Y. Cotte, F. Toy, P. Jourdain, N. Pavillon, D. Boss, P. Magistretti, P. Marquet, and C. Depeursinge, "Marker-free phase nanoscopy," *Nature Photonics* 7, 113-117 (2013).
- [10] D. Kim, S. Lee, M. Lee, J. Oh, S.-A. Yang, and Y. Park, "Refractive index as an intrinsic imaging contrast for 3-D label-free live cell imaging," *bioRxiv*, 106328 (2017).
- [11] S. Shin, K. Kim, T. Kim, J. Yoon, K. Hong, J. Park, Y. Park, "Optical diffraction tomography using a digital micromirror device for stable measurements of 4-D refractive index tomography of cells", *Proc. of SPIE* Vol. 9718, pp. 971814-1, 2016
- [12] H. Irshad, A. Veillard, L. Roux, D. Racoceanu, "Methods for nuclei detection, segmentation, and classification in digital histopathology: a review - current status and future potential", *IEEE reviews in biomedical engineering*, 7, 97-114, 2014
- [13] K. Kim, W. S. PARK, S. Na, S. Kim, T. Kim, W. D. Heo, and Y. Park, "Correlative three-dimensional fluorescence and refractive index tomography: bridging the gap between molecular specificity and quantitative bioimaging," *bioRxiv*, 186734 (2017).
- [14] I. Wolf, M. Vetter, I. Wegner, T. Böttger, M. Nolden, M. Schöbinger, H. P. Meinzer, "The medical imaging interaction toolkit", *Medical image analysis*, 9(6), 594-604, 2005
- [15] J. Kniss, K. Gordon, H. Charles, "Multidimensional transfer functions for interactive volume rendering", *IEEE Transactions on visualization and computer graphics* 8(3), 270-285, 2002
- [16] J. Yoon, Y. Jo, M.-h. Kim, K. Kim, S. Lee, S.-J. Kang, and Y. Park, "Identification of non-activated lymphocytes using three-dimensional refractive index tomography and machine learning," *Scientific Reports* 7(2017).
- [17] K. Kim, S. Lee, J. Yoon, J. Heo, C. Choi, and Y. Park, "Three-dimensional label-free imaging and quantification of lipid droplets in live hepatocytes," *Scientific reports* 6, 36815 (2016).
- [18] C. W. Chen, J. Luo, K. J. Parker, "Image segmentation via adaptive K-mean clustering and knowledge-based morphological operations with biomedical applications", *IEEE transactions on image processing*, 7(12), 1673-1683, 1998